Epidemics with containment measures

Ginestra Bianconi [1,2] and P. L. Krapivsky [3]

[1]*School of Mathematical Sciences, Queen Mary University of London, London E1 4NS, United Kingdom*
[2]*The Alan Turing Institute, 96 Euston Road, London NW1 2DB, United Kingdom*
[3]*Department of Physics, Boston University, Boston, Massachusetts 02215, USA*

We propose a tractable epidemic model that includes containment measures. In the absence of containment measures, the epidemics spread exponentially fast whenever the infectivity rate is positive $\lambda > 0$. The containment measures are modeled by considering a time-dependent modulation of the bare infectivity λ leading to effective infectivity that decays in time for each infected individual, mimicking, for instance, the combined effect of the asymptomatic onset of the disease, testing policies, and quarantine. We consider a wide range of temporal kernels for effective infectivity, and we investigate the effect of the considered containment measures. We find that not all kernels are able to push the epidemic dynamics below the epidemic threshold with some containment measures only able to reduce the rate of the exponential growth of newly infected individuals. We also propose a pandemic model caused by a growing number of separated foci.

I. INTRODUCTION

The world is much more connected than ever. This greatly simplifies the spread of pandemics. On the other hand, the quick introduction of various containment measures [1–3], the wide testing and immunization policies [4–7], and modern ways of analyzing data [8,9] help to fight the pandemics as never before. Here, we introduce and analyze a simple model of epidemic spreading mimicking containment measures that can help to shed light on the dynamics at the onset of a pandemic.

The study of epidemics has a long and fascinating history [10,11]. Epidemic modeling goes back to Bernoulli who modeled the spread of smallpox [12]. The modeling literature grows rapidly as the new challenges ranging from HIV [13,14] and COVID-19 [1–9,15–19] to computer viruses [20] and rumor spreading [21–24] continue to emerge. Epidemic spreading processes are described not only in mathematical biology books [25–29], but also in statistical physics [30], network theory textbooks [31–34], and topical reviews [35]. The susceptible-infected (SI), susceptible-infected-susceptible, and susceptible-infected-recovered (SIR) are especially popular epidemic models. These models have been mostly studied in well-mixed populations where every individual can be in contact with any other [25–29,36], but also on networks [35] or in a metapopulation framework [37] formed by several well-mixed populations interacting through a network [38]. In all these models, when the infectivity λ exceeds the threshold value λ_c, the spread is exponentially fast in time at the onset of the epidemic outbreak [31]. When $\lambda < \lambda_c$, the epidemics quickly die out. The range $\lambda \approx \lambda_c$ is particularly interesting; the behaviors in this regime are not fully understood even in the realm of the classical models, such as SIR [39–46], but, at least, it is well established

that such epidemics cannot affect a finite fraction of the population.

The containment measures successfully stop the spread of the epidemic if they can raise the value of the epidemic threshold to $\lambda_c > \lambda$. For epidemic spreading models defined on networks, the epidemic threshold depends on the network topology [31–35]. Here, we take a well-mixed population approach to model the evolution of a single focus (hot spot) of the epidemics. This is reasonable for airborne diseases spreading through contact networks that are highly random and dense, particularly, in urban centers. The topology of these contact networks is likely to be quite different from the topology of social networks in which links indicate a social tie, and the data about these networks is not very rich with the only exception of studies investigating face-to-face interactions in settings, such as schools or hospitals [47,48].

Here, we study the role of containment measures in mitigating and ultimately halting the epidemics. At the level of a single foci, the containment measures are of two types: Measures that aim to reduce the average number of contacts between individuals of the population, and measures that aim to detect and isolate or cure rapidly the new cases. Although the first class of containment measure strongly depends on the network of contacts, the second class of containment measures only depend on how fast new cases are detected and isolated. In this article, we exclusively consider the latter containment measures. In order to have a simple and analytically tractable model, we neglect the network effects. To model epidemics in the presence of these containment measures, we consider a well-mixed epidemic model in infinite population. We do not intend to model real data; rather, we want to mathematically clarify, in a completely solvable model, how timely detection and isolation of the cases can mitigate or even stop the spread by pushing the dynamics in the subcritical regime.

As in the SIR, we have subpopulations of susceptible individuals, infected individuals who spread the infection, and removed individuals who had the infection, and perhaps still have, but cannot spread it any longer. The epidemic dynamics is very simple as the only relevant transition is from the susceptible to the infected state if it is in contact with an infected individual. At each time step, infected individuals have a nonzero probability to become removed when they are detected and isolated by the tracking of the spread. Thus, on average, the infectivity of infected individuals decreases in time. This suggests to model the effect of different containment measures by introducing a temporal kernel $F(\tau)$ that modulates the infectivity of each infected individual. This kernel results from containment policies aiming to isolate and track cases. In particular, we assume that the effective infectivity $\lambda F(\tau)$ of an infected individual decays with the time τ that has elapsed after the individual got infected. Depending on the functional form of the temporal kernel $F(\tau)$, we investigate the critical properties of the epidemic spreading process, characterize the epidemic threshold of the model with containment measures, and the asymptotic scaling of the number $n(t)$ of infected individuals with time t. We determine when the containment measures are effective in pushing the dynamics in the subcritical regime with $\lambda < \lambda_c$. Additionally, we show that, in the subcritical regime, the total number $N(t)$ of infected individuals is constant asymptotically in time indicating that the spread of the epidemics has been halted. In the critical regime, it is possible to observe a polynomial growth of $N(t)$ of a given epidemic focus. When the containment measures are too mild to achieve the halting of the epidemics, i.e., $\lambda > \lambda_c$, we quantify the impact of the adopted measures in reducing the rate of the exponential growth.

We also briefly examine a multifoci version. We model the geographic spread of the epidemic by assuming that it is caused by the combined effects of different epidemic foci. In real scenarios, one might consider to take into account commuting patterns between the epidemic foci as this is the ultimate cause for the establishment of new foci. Our stylized model neglects the network effects depending on details of the particular situation which are also easily perturbed during the lockdown. We assume, instead, that these commuting patterns have the global effect of increasing the number of epidemic foci in time. Our results show that the total number of cases across different foci of the epidemics can grow either exponentially when the system is in the supercritical regime or as a power law of time if the system is in the critical regime.

The paper is structured as follows. In Sec. II, we show that our single focus epidemic model with containment dynamics captures the average behavior of an underlying stochastic model. We also list the temporal kernels $F(\tau)$ that we use to mimic the containment measures. In Sec. III, we provide the exact solution of the model for an arbitrary kernel $F(\tau)$ using the generating function formalism. In Secs. IV–VII, we discuss in detail the solution of the model for the four considered temporal kernels: the constant kernel, the power-law kernel, the exponential kernel, and the generalized exponential kernel; in Sec. VIII, we discuss the multifoci generalization of the SI dynamics. In Sec. IX, we characterize the total number of infected individuals in the multifoci model. Conclusions are

presented in Sec. X. Some details of calculations are relegated to the Appendices.

II. SINGLE FOCUS EPIDEMIC MODEL WITH CONTAINMENT DYNAMICS

A. Underlying stochastic model

In a typical SIR epidemic model, the infectivity λ of an infected individual does not change with time as long as the infected individual is contagious. It is also assumed that each infected individual is removed from the population with a probability that does not depend on time. Therefore, in the SIR model in the well-mixed infinite population limit, the density of infected individuals increases exponentially in the supercritical regime.

Here, we consider an alternative approach and study a model in which an infected individual has a reproductive number that changes with time starting from the time τ counted from the moment when an individual has become infectious. The constant infectivity λ is, thus, replaced by time-dependent infectivity,

$$\lambda \rightarrow \lambda F(\tau), \tag{1}$$

where $F(\tau)$ is a decreasing function of τ. This decay of the effective infectivity can be due to different causes including asymptomatic onset, early testing policies, and containment measures enforced once the infection becomes symptomatic.

To motivate this model, we mention a specific stochastic model whose average behavior is captured by the dynamics of our model. Consider an individual infected at time $\tau = 0$. At time step $\tau > 0$, this individual can be removed from the population (meaning isolation, recovery, or death) with probability $p(\tau)$. Therefore, the probability that, at time τ, the individual is still infecting other individuals in the population is

$$P(\tau) = \prod_{\tau'=1}^{\tau} p(\tau'). \tag{2}$$

Additionally, we assume that, at time τ, an infected and not yet removed individual infects in average $\lambda m(\tau)$ other individuals. In this stochastic model in the infinite population limit, an individual infected at time $\tau = 0$ infects, on average,

$$\lambda F(\tau) = \lambda P(\tau) m(\tau), \tag{3}$$

other individuals at time $\tau > 0$. It follows that $F(\tau)$ acts as an overall dressing of the infectivity that captures timely detection, tracking, and isolation.

B. Deterministic model

In this paper, we focus on the deterministic version of the model discussed in the previous paragraph. Starting at time $t = 0$ from a single infected individual $n(0) = 1$, the average number $n(t)$ of individuals infected at time $t \geqslant 1$ is given by

$$n(t) = \lambda \sum_{t'=0}^{t-1} F(t - t') \, n(t'), \tag{4}$$

where $F(\tau)$ is the temporal kernel that describes how the effective infectivity of an infected individual decays as a function of time τ elapsed since his infection. This equation is called the renewal equation. In addition to $n(t)$, we analyze the behavior of the total number $N(t)$ of individuals infected up to time t,

$$N(t) = \sum_{t'=0}^{t} n(t').$$ (5)

We consider the following temporal kernels $F(\tau)$:

(1) *Constant kernel.*

In this case, the effective infectivity of an infected individual remains constant in time,

$$F(\tau) = 1.$$ (6)

In this case, there are no containment measures, and the epidemic model reduces to the standard SI model.

(2) *Power-law kernel.*

In this case, the effective infectivity of an infected individual decays as a power law of time,

$$F(\tau) = \frac{1}{\tau^\alpha},$$ (7)

with $\alpha \geqslant 0$. For $\alpha = 0$, we recover the constant kernel.

(3) *Exponential kernel.*

In this case, the effective infectivity of an an infected individual decays exponentially in time,

$$F(\tau) = \exp[-\gamma\tau],$$ (8)

with $\gamma \geqslant 0$. For $\gamma = 0$, we recover the constant kernel.

(4) *Generalized exponential kernel.*

In this case, the effective infectivity of an an infected individual decays in time as

$$F(\tau) = \exp[-\gamma\tau^b],$$ (9)

with $\gamma > 0$. For $b = 1$, we recover the exponential kernel. For $b > 1$, the decay of this temporal kernel is faster than exponential, and for $b < 1$, it is slower than exponential.

III. GENERAL SOLUTION OF THE SINGLE FOCUS MODEL

A. Exact solution

The best way of analyzing recurrences, such as Eq. (4) is via generating functions. Indeed, the generating function,

$$\mathcal{N}(x) = \sum_{t \geqslant 0} n(t) x^t$$ (10)

converts the recurrence Eq. (4) into a linear equation for the generating function,

$$\mathcal{N}(x) = 1 + \lambda \mathcal{F}(x) \mathcal{N}(x),$$ (11)

with

$$\mathcal{F}(x) = \sum_{\tau \geqslant 1} F(\tau) x^\tau$$ (12)

being the generating function of the temporal kernel. Hence, Eq. (10) admits the solution,

$$\mathcal{N}(x) = \frac{1}{1 - \lambda \mathcal{F}(x)}.$$ (13)

The generating function $\mathcal{F}(x)$ is well defined for $x < R$, where R is the radius of convergence. The convergence radius has an obvious lower bound, $R \geqslant 1$, in the relevant situations when the temporal rate $F(\tau)$ is a nonincreasing function of τ.

The generating function $\mathcal{N}(x)$ typically has a pole at a certain $x = e^{-\mu} < R$. The location of the pole is found from

$$\lambda \mathcal{F}(e^{-\mu}) = 1.$$ (14)

The pole must be simple since $\mathcal{F}(x)$ is a strictly increasing function of x, in the nonpathological case when $F(\tau) \geqslant 0$. Applying the theorem of residues to Eq. (13), we deduce the exponential asymptotic,

$$n(t) \simeq A_\mu e^{\mu t}$$ (15)

for $t \gg 1$, with growth rate μ determined by Eq. (14) and,

$$A_\mu = e^\mu \frac{\mathcal{F}(e^{-\mu})}{\mathcal{F}'(e^{-\mu})},$$ (16)

where $\mathcal{F}' = \frac{d\mathcal{F}}{dx}$. If the condition $x = e^{-\mu} < R$ is valid, and $\mu > 0$, the number of newly infected individuals grows exponentially with time t; for $\mu = 0$, it remains constant in time; if $\mu < 0$, it decays exponentially with time. In the interesting regimes with $\mu \geqslant 0$, the total number of infected individuals $N(t)$ grows as

$$N(t) \simeq \begin{cases} A_\mu (e^\mu - 1)^{-1} e^{\mu t}, & \mu > 0, \\ A_0 t, & \mu = 0. \end{cases}$$ (17)

When $\mu < 0$, the total number of infections saturates.

Thus, if the growth rate of new infections is positive, $\mu > 0$, the total number of infected individuals grows exponentially in time at the same rate as the number of new infections. In the critical case $\mu = 0$, the total number of infected individuals $N(t)$ increases linearly with time. The amplitude in this situation has a neat form

$$A_0 = \frac{\mathcal{F}(1)}{\mathcal{F}'(1)} = \frac{\displaystyle\sum_{\tau \geqslant 1} F(\tau)}{\displaystyle\sum_{\tau \geqslant 1} \tau F(\tau)}.$$ (18)

If the condition $x = e^{-\mu} < R$ is no longer valid, the scaling of the number $n(t)$ of newly infected individuals and the scaling of the total number $N(t)$ of infected individuals can deviate significantly from the exponential behavior indicated in Eqs. (15) and (17), respectively. Explicit cases where these deviations are observed will be discussed in detail in the next sections.

In this article, we employ the discrete-time formulation. We remark that the renewal equation can be defined in the continuous time framework, and it is amenable to an exact analytic solution by making use of Lagrange transforms rather than generating functions.

B. Epidemic threshold and dynamical regimes

From the exact solution of $\mathcal{N}(x)$ given by Eq. (13), we deduce that the SI epidemic model defined by Eq. (4) has the epidemic threshold given by

$$\lambda_c = \lim_{x \to 1^-} \frac{1}{\mathcal{F}(x)}. \tag{19}$$

Equation (13) further implies that our epidemic model exhibits different behaviors depending on whether λ is larger, equal, or smaller than λ_c.

In the *supercritical regime* $\lambda > \lambda_c$, the generating function $\mathcal{N}(x)$ given by Eq. (14) has a simple pole at $x = e^{-\mu}$ with $\mu > 0$. Hence, the number of newly infected individuals exhibits a purely exponential asymptotic growth. In some special cases, it is possible to get exact results $n(t)$. For instance, for the constant kernel and exponential kernels, the exponential behavior is exact, i.e., valid for all $t \geqslant 1$.

The rate μ approaches to zero when $\lambda \to \lambda_c^+$. The behavior is particularly simple when $\mathcal{F}(x)$ is differentiable at $x = 1$ so that the zeroth and first moments of the temporal rate $F(\tau)$ are well defined, i.e., $\mathcal{F}(1)$ and $\mathcal{F}'(1)$ are finite. In this situation, we expand Eq. (14) and find

$$\mu \simeq D(\lambda - \lambda_c), \tag{20}$$

with neat general expressions for the epidemic threshold λ_c and amplitude D,

$$\lambda_c = \frac{1}{\mathcal{F}(1)}, \qquad D = \frac{1}{\lambda_c^2 \mathcal{F}'(1)}. \tag{21}$$

For temporal kernels with the radius of convergence $R = 1$ and $\mathcal{F}'(1) = \infty$, the behavior of μ in the $\lambda \to \lambda_c^+$ limit can be more surprising. In the majority of cases, we have observed an algebraic behavior,

$$\mu \simeq D(\lambda - \lambda_c)^\beta \tag{22}$$

characterized by the *dynamical exponent* $\beta \geqslant 1$. Alternatively, the linear scaling law (20) can acquire a logarithmic correction.

The *critical regime* $\lambda = \lambda_c$, separates the supercritical regime from the subcritical regime. If $R > 1$, then $n(t)$ saturates according to Eq. (15). If $R = 1$, the asymptotic behavior of $n(t)$ can be extracted from an asymptotic expansion of $\mathcal{N}(x)$ for $0 < 1 - x \ll 1$; the emerging asymptotic behavior of $n(t)$ could be rich and varied depending on the kernel $F(\tau)$ as we will demonstrate in the following sections.

In the *subcritical regime* $\lambda < \lambda_c$, the number of new infections decreases with time. Indeed, the generating function $\mathcal{N}(x)$ remains finite at $x = 1$,

$$\mathcal{N}(1) = \frac{1}{1 - \lambda/\lambda_c} < \infty. \tag{23}$$

By definition,

$$\mathcal{N}(1) = \sum_{t \geqslant 0} n(t), \tag{24}$$

so the number of new infections $n(t)$ converges to zero,

$$\lim_{t \to \infty} n(t) = 0. \tag{25}$$

If $R = \infty$, the number of new infections $n(t)$ exhibits an asymptotic exponential decay according to Eq. (15). When the convergence radius is finite and obeys $R > 1$, more complicated behaviors can occur as we will demonstrate.

The definition of our epidemic spreading model implies that the number of newly infected individuals $n(t)$ cannot decay faster than $F(t)$. Indeed, Eq. (4) yields

$$n(t) = \sum_{t'=1}^{t-1} F(t - t')n(t')$$

$$= n(1)F(t - 1) + n(2)F(t - 2) + \cdots, \tag{26}$$

and truncating the sum at the first term, we have

$$n(t) \geqslant F(t - 1) \simeq F(t) \tag{27}$$

for $t \gg 1$.

In the following sections, we demonstrate how the general exact approach described above applies to the four kernels we analyze in detail. We will show that, if there are no containment measures, $F(\tau) = 1$, the exponential growth emerges for any $\lambda > 0$. Thus, for the constant kernel, the model reduces to the SI model, and it is always in the supercritical regime. We will also show that containment measures modeled by sufficiently quickly decaying kernels $F(\tau)$ can be efficient in containing the epidemic spread by pushing the dynamics in the subcritical regime. Less stringent containment measures are not always able to drive the model in the subcritical regime, and they merely decrease the rate μ of the exponential growth.

IV. CONSTANT KERNEL

For the constant kernel $F(\tau) = 1$, Eq. (4) becomes

$$n(t) = \lambda \sum_{t'=0}^{t-1} n(t'). \tag{28}$$

The initial condition is $n(0) = 1$. Equation (28) can be also written as

$$n(t) = (1 + \lambda)n(t - 1), \tag{29}$$

which is solved to yield

$$n(t) = \lambda(1 + \lambda)^{t-1} = \frac{\lambda}{1 + \lambda} e^{\mu t}, \tag{30}$$

with

$$\mu = \ln(1 + \lambda). \tag{31}$$

For any infectivity $\lambda > 0$, the rate μ is always positive. The number of new infections $n(t)$ exhibits a pure exponential growth. The total number of infected individuals $N(t)$ also grows exponentially with time,

$$N(t) = \sum_{t'=0}^{t} n(t') = (1 + \lambda)^t = e^{\mu t}. \tag{32}$$

Therefore, for any $\lambda > 0$, the system is in the supercritical regime.

The above qualitative predictions can be also deduced from our general formalism. Indeed, for the constant kernel $F(\tau) =$

1, we have $\mathcal{F}(x) = \frac{x}{1-x}$, and Eq. (19) implies that the epidemic threshold is vanishing: $\lambda_c = 0$. We also note that, for $0 < \lambda \ll 1$, the exponential rate μ given by Eq. (31) is asymptotically

$$\mu = \lambda + O(\lambda^2). \tag{33}$$

Thus, the rate μ follows the power-law scaling (22) with $\lambda_c = 0$, $D = 1$, and $\beta = 1$.

V. POWER-LAW KERNEL

The power-law kernel exemplifies kernels with a slow decay in time. Below, we show that, for $\alpha \leqslant 1$, the epidemic threshold vanishes, $\lambda_c = 0$, and $n(t)$ exhibits an exponential asymptotic growth for any value of $\lambda > \lambda_c = 0$. Therefore, the containment measures can be effective in pushing the dynamics in the subcritical regime only if $\alpha > 1$. For any $\alpha > 1$, the epidemic threshold is, indeed, positive, $\lambda_c > 0$, so the containment measures bring the epidemics to the subcritical regime when $\lambda < \lambda_c$.

A. Epidemic threshold

We tacitly assume that $\alpha > 0$ since $\alpha = 0$ reduces to the constant kernel. When $F(\tau) = \tau^{-\alpha}$, the generating function $\mathcal{F}(x)$ is a polylogarithmic function of order α,

$$\mathcal{F}(x) = \mathrm{Li}_\alpha(x) = \sum_{n \geqslant 1} \frac{x^n}{n^\alpha}. \tag{34}$$

According to the general solution of the model given in Sec. III A, the generating function $\mathcal{N}(x)$ becomes

$$\mathcal{N}(x) = \frac{1}{1 - \lambda \, \mathrm{Li}_\alpha(x)}, \tag{35}$$

and the epidemic threshold of this model is given by

$$\lambda_c = \lim_{x \to 1^-} \frac{1}{\mathrm{Li}_\alpha(x)}. \tag{36}$$

Figure 1 shows the plot of the epidemic threshold λ_c versus the power-law exponent α.

Since $\mathrm{Li}_\alpha(x)$ diverges at $x = 1$ when $\alpha \leqslant 1$, we conclude that $\lambda_c = 0$ when $0 \leqslant \alpha \leqslant 1$. The most gentle logarithmic divergence occurs in the marginal case of $\alpha = 1$ when $\mathrm{Li}_1(x) = -\ln(1 - x)$. Thus, for any $\lambda > 0$, the epidemic is in the supercritical regime when $0 < \alpha \leqslant 1$. According to Eq. (15), the number $n(t)$ of new infected individuals grows exponentially with time at rate $\mu > 0$ given by Eq. (14). The larger the decay exponent α, the more stringent are the containment measures, so the rate μ is a decreasing function of α. Hence, for $0 < \alpha < 1$, the containment measures mitigate the spread of the epidemics but cannot stop its exponential growth.

For $\alpha > 1$, the epidemic threshold is finite,

$$\lambda_c = \frac{1}{\mathrm{Li}_\alpha(1)} = \frac{1}{\zeta(\alpha)} > 0, \tag{37}$$

where $\zeta(\alpha) = \sum_{n \geqslant 1} n^{-\alpha}$ is the ζ function. Thus, for $\lambda < \lambda_c$, the containment measures push the dynamics in the subcritical regime stopping the exponential growth. Since $\zeta(\alpha) > 1$ for all $\alpha > 1$, the epidemic threshold λ_c is bounded from above, viz.,
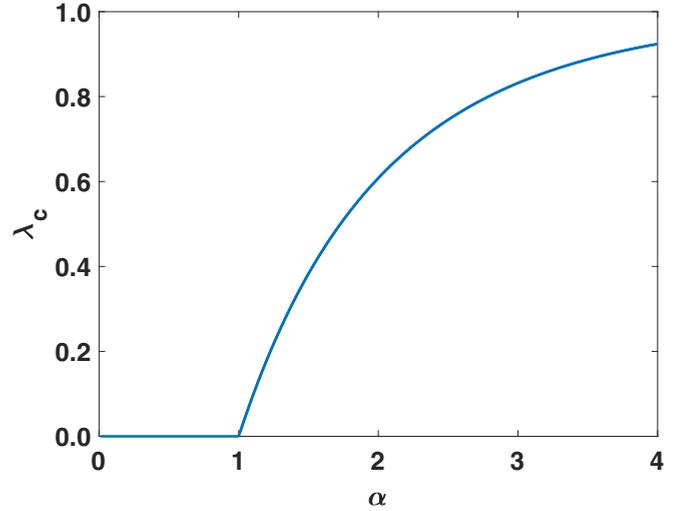
$$\lambda_c < 1. \tag{38}$$

FIG. 1. The epidemic threshold λ_c versus the exponent α characterizing the power-law kernel (7). The epidemic threshold vanishes, $\lambda_c = 0$, for $0 < \alpha \leqslant 1$; when $\alpha > 1$, the epidemic threshold is an increasing function of α obeying $\lambda_c \leqslant 1$.

The ζ function has a simple pole at $\alpha = 1$, and near the pole, it admits an expansion,

$$\zeta(\alpha) = \frac{1}{\alpha - 1} + \gamma_E + O(\alpha - 1), \tag{39}$$

where $\gamma_E = 0.5772\,156\,649 \cdots$ is the Euler-Mascheroni constant. Using this expansion, one deduces the scaling of the epidemic threshold when $0 < \alpha - 1 \ll 1$,

$$\lambda_c = \alpha - 1 - \gamma_E(\alpha - 1)^2 + O[(\alpha - 1)^3]. \tag{40}$$

We now discuss, in detail, the supercritical, critical, and subcritical regimes for the power-law kernel with decay exponent $\alpha > 0$.

B. Supercritical regime

The general solution of the model, Sec. III A, implies that, in the supercritical regime, the number of individuals infected at time t obeys the asymptotic scaling,

$$n(t) \simeq A_\mu e^{\mu t}, \tag{41}$$

with $\mu > 0$ satisfying Eq. (14) which becomes

$$1 = \lambda \, \mathrm{Li}_\alpha(e^{-\mu}). \tag{42}$$

The amplitude A_μ in (41) is given by (16) which gives

$$A_\mu = e^\mu \frac{\mathrm{Li}_\alpha(e^{-\mu})}{\mathrm{Li}_{\alpha-1}(e^{-\mu})}. \tag{43}$$

In Fig. 2(a), we provide numerical evidence of the exponential grow of $n(t)$ in the supercritical regime $\lambda > \lambda_c$. Both $n(t)$ and $N(t)$ exhibit the exponential growth with the same growth rate and only amplitudes differ,

$$N(t) \simeq C e^{\mu t}, \tag{44}$$
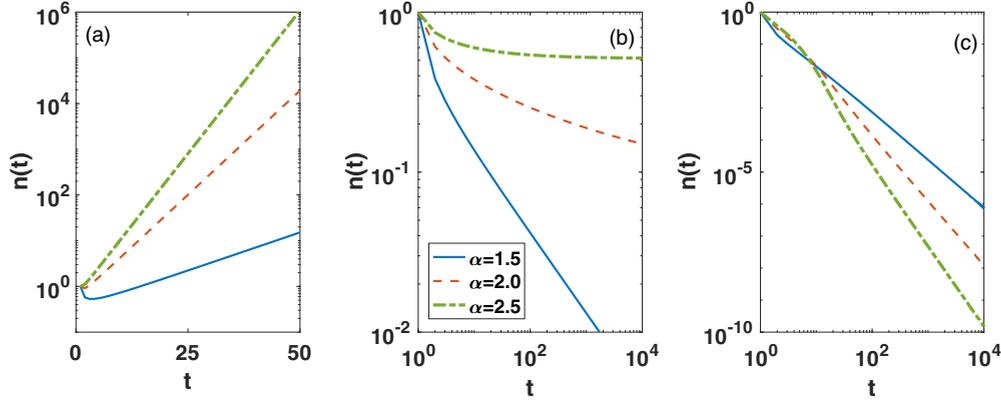
with $C = A_\mu / (e^\mu - 1)$.

FIG. 2. The number $n(t)$ of newly infected individuals for the power-law kernel (7) is plotted versus time t for $\alpha = 1.5, 2.0, 2.5$. Panel (a) refers to the supercritical regime with $\lambda = 1.5\lambda_c$; panel (b) refers to the critical regime with $\lambda = \lambda_c$; panel (c) refers to the subcritical regime with $\lambda = 0.5\lambda_c$.

The growth rate $\mu > 0$ depends on α and λ. For $\alpha \neq 1$, the rate μ is implicitly determined by Eq. (42). This transcendental equation does not admit a general explicit solution. One exception is the marginal case of $\alpha = 1$ when the polylogarithmic function becomes $\mathrm{Li}_1(x) = -\ln(1 - x)$. Combining this with Eq. (42), we extract an explicit expression,

$$\mu = -\ln(1 - e^{-1/\lambda}), \qquad (45)$$

in the marginal case of $\alpha = 1$.

We now present various asymptotic expansions of μ for different values of α. In particular, we analyze the scaling of μ for $\lambda \to \infty$ and for $\lambda \to \lambda_c^+$ at $\alpha \geqslant 0$.

1. Scaling of μ for $\lambda \to \infty$

For the constant temporal kernel, the growth rate reads $\mu = \ln(1 + \lambda)$, see Eq. (31), so it diverges logarithmically as $\lambda \to \infty$. The presence of nontrivial power-law containment measures ($\alpha > 0$), the rate μ also diverges logarithmically as we now demonstrate. Indeed, combining the definition (34) of the polylogarithmic function,

$$\mathrm{Li}_\alpha(e^{-\mu}) = e^{-\mu} + 2^{-\alpha}e^{-2\mu} + \cdots,$$

with Eq. (42), we find

$$\mu = \ln(1 + \lambda) - \frac{1 - 2^{-\alpha}}{\lambda} + O(\lambda^{-2}). \qquad (46)$$

This analytical prediction is supported by numerical results, see Fig. 3 where we plot $\ln(1 + \lambda) - \mu$ versus α. In the limit $\lambda \to \infty$, we observe the same leading term as for $\alpha = 0$ with an α-dependent subleading correction of order of $1/\lambda$. Thus, the containment measures lead only to subleading corrections to a diverging value of μ.

2. Scaling of μ when $\lambda \to \lambda_c^+$

Here, we examine the behavior of the growth rate μ in the $\lambda \to \lambda_c^+$ limit. The linear scaling (20) occurs when $\alpha > 2$. A more general scaling law (22) with dynamical exponent $\beta > 1$ occurs in the range of $0 < \alpha < 2$. There are two anomalies: when $\alpha = 1$, the exponent β diverges, whereas when $\alpha = 2$, there is an additional logarithmic correction to the linear scaling (20). These scalings are summarized in Table I. We

now derive these results and establish the dependence of the amplitude D and the exponent β on α.

(a) *The case of $0 \leqslant \alpha < 1$.*

From the definition (34) of the polylogarithmic function, one extracts the expansion,

$$\mathrm{Li}_\alpha(x) = (1 - x)^{\alpha-1}\Gamma(1 - \alpha) + O(1), \qquad (47)$$

when $x \to 1^-$. Substituting this expansion into Eq. (42), we obtain

$$\mu \simeq D\lambda^{1/(1-\alpha)}, \qquad D = [\Gamma(1 - \alpha)]^{1/(1-\alpha)}. \qquad (48)$$

Thus, $\lambda_c = 0$ and $\beta = (1 - \alpha)^{-1}$.

(b) *The case of $\alpha = 1$.*

The epidemic threshold also vanishes in this case, $\lambda_c = 0$, and the explicit solution (45) leads to the exponential scaling,

$$\mu = e^{-1/\lambda} + O(e^{-2/\lambda}). \qquad (49)$$

Thus, the exponent β is effectively infinite.

(c) *The case of $1 < \alpha < 2$.*

The epidemic threshold is $\lambda_c = 1/\zeta(\alpha)$. The polylogarithmic function admits the asymptotic expansion,

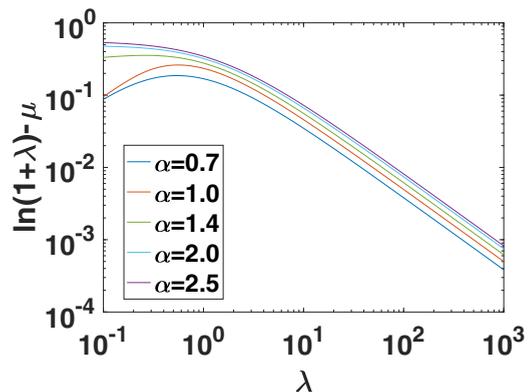$$\mathrm{Li}_\alpha(x) = \zeta(\alpha) + (1 - x)^{\alpha-1}\Gamma(1 - \alpha) + \cdots, \qquad (50)$$

FIG. 3. The discrepancy $\ln(1 + \lambda) - \mu$ between the growth rate μ and its universal leading behavior is plotted versus λ for the model with power-law kernel (7). The results for different values of the exponent $\alpha = 0.7, 1.0, 1.4, 2.0, 2.5$ are shown.

TABLE I. The growth rate μ characterizing the exponential asymptotic behavior of the number of infected individuals $n(t) \sim e^{\mu t}$ for the power-law kernel $F(\tau) = 1/\tau^\alpha$ in the supercritical regime $\lambda > \lambda_c$.

α	$0 < \alpha < 1$	$\alpha = 1$	$1 < \alpha < 2$	$\alpha = 2$	$\alpha > 2$
μ	$D\lambda^{1/(1-\alpha)}$	$e^{-(1/\lambda)}$	$D(\lambda - \lambda_c)^{1/(\alpha-1)}$	$-D(\lambda - \lambda_c)/|\ln(\lambda - \lambda_c)|$	$D(\lambda - \lambda_c)$

when $x \to 1^-$. By inserting this expansion into Eq. (42), we arrive at Eq. (22) with

$$\beta = \frac{1}{\alpha - 1}, \qquad D = \left[-\frac{\zeta^2(\alpha)}{\Gamma(1-\alpha)} \right]^{1/(1-\alpha)}. \tag{51}$$

(d) *The case of $\alpha = 2$.*

The polylogarithmic function $\mathrm{Li}_2(x)$ admits the asymptotic expansion,

$$\mathrm{Li}_2(x) = \zeta(2) + (1-x)[\ln(1-x) - 1] + \cdots \tag{52}$$

when $x \to 1^-$. By inserting Eq. (52) into Eq. (42) and recalling that $\lambda_c = 1/\zeta(2) = 6/\pi^2$, we get

$$\mu \simeq -D \frac{(\lambda - \lambda_c)}{\ln(\lambda - \lambda_c)}, \quad D = \zeta^2(2) = \frac{\pi^4}{36}. \tag{53}$$

Thus, when $\alpha = 2$, the rate μ acquires a logarithmic correction to the linear in $\lambda - \lambda_c$ scaling.

(e) *The case of $\alpha > 2$.*

From the definition (34) of the polylogarithmic function, one extracts the expansion,

$$\mathrm{Li}_\alpha(x) = \zeta(\alpha) - (1-x)\zeta(\alpha - 1) + o(1-x). \tag{54}$$

Inserting this expression into Eq. (42), we find

$$\mu \simeq D(\lambda - \lambda_c), \qquad D = \frac{\zeta^2(\alpha)}{\zeta(\alpha - 1)}. \tag{55}$$

Thus, the dynamical exponent is universal $\beta = 1$ for all $\alpha > 2$. The prediction (55) can be also deduced by specializing the general result (21) to the power-law kernel with $\alpha > 2$.

Figure 4 shows numerical results providing evidence for the asymptotic scaling behaviors of the growth rate μ as a function of $\lambda - \lambda_c$ discussed above.

C. Critical region: $\alpha > 1$ and $\lambda = \lambda_c$

An asymptotic analysis (see Appendix A for details) shows that at the epidemic threshold $\lambda = \lambda_c = 1/\zeta(\alpha)$, the number of newly infected individuals $n(t)$ exhibits the following asymptotic behaviors:

$$n(t) \simeq \begin{cases} At^{\alpha-2}, & \text{for } 1 < \alpha < 2, \\ A/\ln t, & \text{for } \alpha = 2, \\ A, & \text{for } \alpha > 2. \end{cases} \tag{56}$$

The amplitude A in Eq. (56) actually depends on α,

$$A = \begin{cases} -\zeta(\alpha)/[\Gamma(\alpha - 1)\Gamma(1 - \alpha)], & \text{for } 1 < \alpha < 2, \\ \zeta(2), & \text{for } \alpha = 2, \\ \zeta(\alpha)/\zeta(\alpha - 1), & \text{for } \alpha > 2. \end{cases} \tag{57}$$

Thus, the average number of new cases remains constant when $\alpha > 2$; otherwise, the number of newly infected individuals decays with time. The predictions of Eq. (56) are confirmed by the direct numerical integration of the dynamics dictated by Eq. (4) in the critical regime $\lambda = \lambda_c$, see Fig. 2(b). By using the asymptotic expression for $n(t)$ in Eq. (56), we deduce the

scaling of the total number $N(t)$ of infected individuals at time t, given by

$$N(t) \simeq \begin{cases} Ct^{\alpha-1}, & \text{for } 1 < \alpha < 2, \\ Ct/\ln t, & \text{for } \alpha = 2, \\ Ct, & \text{for } \alpha > 2, \end{cases} \tag{58}$$

with

$$C = \begin{cases} \zeta(\alpha)/[\Gamma(\alpha - 1)\Gamma(2 - \alpha)], & \text{for } 1 < \alpha < 2, \\ \zeta(2), & \text{for } \alpha = 2, \\ \zeta(\alpha)/\zeta(\alpha - 1), & \text{for } \alpha > 2. \end{cases} \tag{59}$$

Thus, in the critical regime, $\lambda = \lambda_c$ with $\alpha > 1$, the total number of infected individuals grows linearly in time when $\alpha > 2$ and sublinearly when $1 < \alpha \leqslant 2$.

D. Subcritical region: $\alpha > 1$ and $\lambda < \lambda_c$

In this subcritical regime, the asymptotic behavior of newly infected individuals is algebraic,

$$n(t) \simeq At^{-\alpha}, \quad A = \frac{\lambda}{[1 - \lambda \zeta(\alpha)]^2}. \tag{60}$$

Thus, the asymptotic behavior is dominated by the time dependence of the power-law kernel $F(\tau)$. One can establish (60) by performing an asymptotic analysis of the behavior of $\mathcal{N}(x)$ as $x \to 1^-$, which, in turn, requires the knowledge of
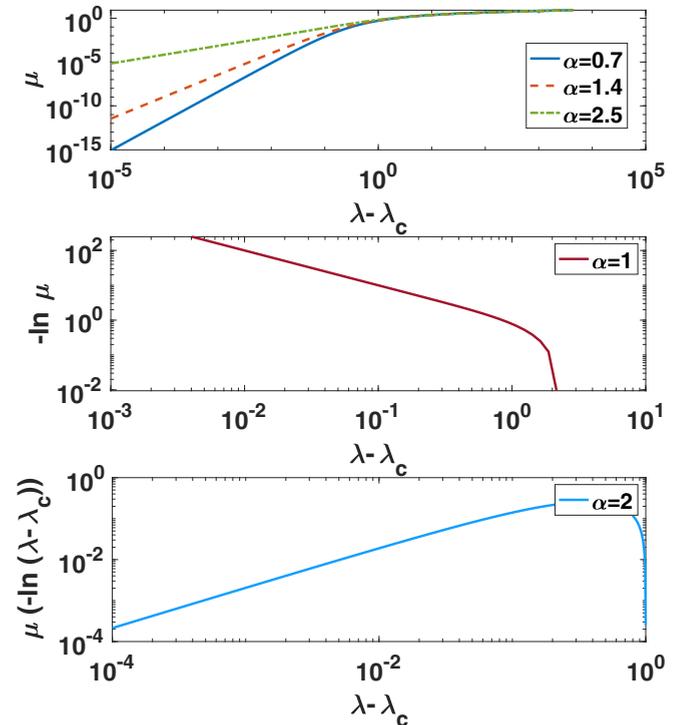
FIG. 4. The growth rate μ versus $\lambda - \lambda_c$ for the power-law kernel (7) with different values of the exponent α.

the behavior of $\mathrm{Li}_\alpha(x)$ as $x \to 1^-$. The details are presented in Appendix B. The analysis is rather straightforward in the range of $1 < \alpha \leqslant 2$ but becomes more and more tedious as the exponent α increases. We have verified (60) in detail when $\alpha < 3$, and we have argued for the validity of the simple general prediction (60), although our proof quickly becomes unwieldy, e.g., it requires the asymptotic expansion until order k and k fold differentiations when $k < \alpha \leqslant k + 1$. Our numerical results, see Fig. 2(c), are in excellent agreement with the theoretical prediction (60) for all values $\alpha > 2$ where we have performed simulations.

Using Eq. (60), we find that the total number of infected individuals $N(t)$ saturates to a constant value,

$$N(t) = A\left[\zeta(\alpha) - \frac{1}{\alpha - 1}t^{1-\alpha}\right] + O(t^{-\alpha}). \quad (61)$$

VI. EXPONENTIAL KERNEL

Let us assume that the effective infectivity of an individual decays exponentially with time $F(\tau) = e^{-\gamma\tau}$. The constant kernel corresponds to $\gamma = 0$, so we tacitly assume that $\gamma > 0$. Equation (4) can be written as the recurrence,

$$n(t) = e^{-\gamma}(1 + \lambda)n(t - 1) \quad (62)$$

valid for any $t \geqslant 2$ with initial condition $n(1) = \lambda e^{-\gamma}$. The solution to the above recurrence reads

$$n(t) = \frac{\lambda}{1 + \lambda}e^{\mu t}, \quad (63)$$

with

$$\mu = \ln(1 + \lambda) - \gamma. \quad (64)$$

For the exponential kernel, the generating function,

$$\mathcal{F}(x) = G_\gamma(x) = \sum_{m=1}^{\infty}(xe^{-\gamma})^m = \frac{e^{-\gamma}x}{1 - xe^{-\gamma}} \quad (65)$$

has the radius of convergence $R = e^\gamma > 1$. The epidemic threshold is

$$\lambda_c = \frac{1}{G_\gamma(1)} = e^\gamma - 1. \quad (66)$$

Thus, the containment measures suppress the spreading of the epidemic when $\lambda < \lambda_c = e^\gamma - 1$.

We, now, use Eqs. (64) and (66) to derive the properties of the three different regimes. In the supercritical phase $\lambda > \lambda_c$, the growth rate (64) is smaller than for the constant kernel (corresponding to $\gamma = 0$). Close to the critical point, the scaling of μ is similar to the scaling in for the constant kernel, namely, it is linear in $\lambda - \lambda_c$,

$$\mu = D(\lambda - \lambda_c), \qquad D = e^{-\gamma}. \quad (67)$$

In the critical phase, the number of new cases is constant in time. In the subcritical phase, the number of new cases decays exponentially. The total number $N(t)$ of infected individuals is determined by Eq. (17) for any value of λ with μ given by Eq. (64).

The scalings of the total number $N(t)$ of infected individuals in the supercritical, critical, and subcritical regimes are summarized in Table II.

TABLE II. Scaling of the total number of infected individuals $N(t)$ for the power-law kernel and for the generalized exponential kernel. Here, $\omega \in (0, 1)$ is an exponent depending on the value of α with $\omega = \alpha - 1$ for $\alpha \in (1, 2)$ and $\omega = 1$ for $\alpha > 2$. The constant C also depends on parameters. For the power-law kernel $F(\tau) = 1/\tau^\alpha$ with $\alpha = 2$, the critical behavior develops a logarithmic correction defined in Eq. (58) and not captured by the present table.

Kernel	$\lambda > \lambda_c$	$\lambda = \lambda_c$	$\lambda < \lambda_c$
$F(\tau) = 1/\tau^\alpha$	$Ce^{\mu t}$	Ct^ω	C
$F(\tau) = \exp(-\gamma\tau^\beta)$	$Ce^{\mu t}$	Ct	C

VII. GENERALIZED EXPONENTIAL DECAY

In this section, we consider a two-parameter class of generalized exponential decay kernels,

$$F(\tau) = \exp[-\gamma\tau^b], \qquad \gamma > 0 \quad \text{and} \quad b > 0. \quad (68)$$

In this case, the generating function $\mathcal{F}(x)$ becomes

$$\mathcal{F}(x) = G_{\gamma,b}(x) = \sum_{m \geqslant 1} x^m e^{-\gamma m^b}. \quad (69)$$

From the general solution presented in Sec. III A, we find that the generating function $\mathcal{N}(x)$ of the number of new infected individuals reads

$$\mathcal{N}(x) = \frac{1}{1 - \lambda\, G_{\gamma,b}(x)}, \quad (70)$$

and the epidemic threshold is given by

$$\lambda_c = \frac{1}{G_{\gamma,b}(1)} = \left[\sum_{m=1}^{\infty} e^{-\gamma m^b}\right]^{-1}. \quad (71)$$

In Fig. 5, we plot the epidemic threshold λ_c as a function of b for generalized exponential kernels with $\gamma = 1$.

For all $b > 0$, values of $G_{\gamma,b}(1)$ and $G'_{\gamma,b}(1)$ are finite, therefore, the growth rate μ exhibits the linear scaling (20) and (21) in the $\lambda \to \lambda_c^+$ limit. Specializing Eq. (21) to the kernel
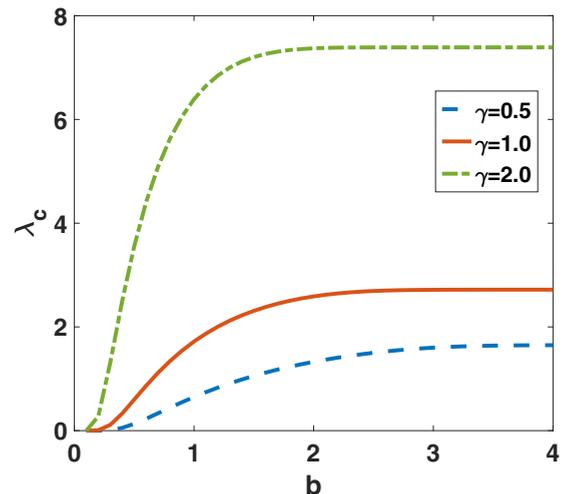

FIG. 5. The epidemic threshold λ_c for generalized exponential kernel (68) is plotted versus b for $\gamma = 0.5, 1.0, 2.0$.
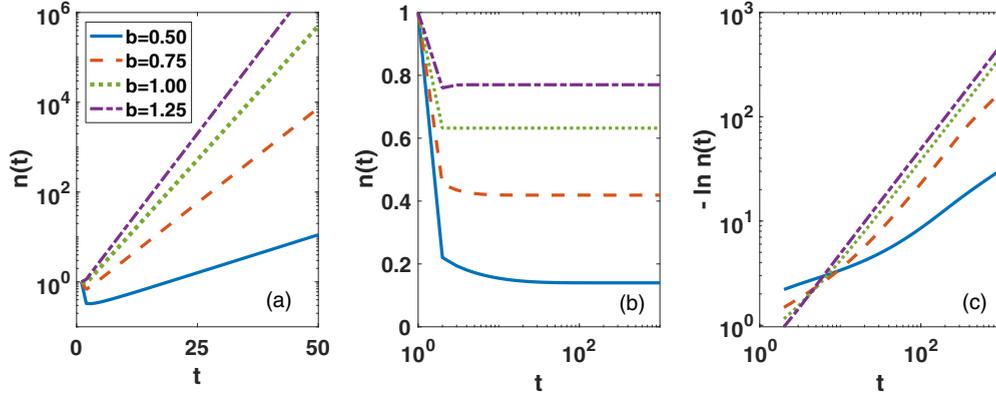
FIG. 6. The number $n(t)$ of newly infected individuals is plotted versus time t for the generalized exponential kernel $F(\tau)$ given by Eq. (68) with $\gamma = 1$ and $b = 0.50, 0.75, 1.00, 1.25$. Panel (a) refers to the supercritical regime with $\lambda = 1.5\lambda_c$, panel (b) refers to the critical regime $\lambda = \lambda_c$, and panel (c) refers to the subcritical regime $\lambda = 0.5\lambda_c$.

(68), we get Eq. (71) with

$$D = \frac{[G_{\gamma,b}(1)]^2}{G'_{\gamma,b}(1)} = \frac{\left[\sum_{m \geqslant 1} e^{-\gamma m^b}\right]^2}{\sum_{m \geqslant 1} m e^{-\gamma m^b}}. \quad (72)$$

The sums appearing in Eqs. (71) and (72) cannot be generally expressed through known special functions. One exception is the $b = 2$ case when recalling the definition of the Jacobi θ function,

$$\theta_3(q) = \sum_{n=-\infty}^{\infty} q^{n^2}, \quad (73)$$

we rewrite the epidemic threshold as

$$\lambda_c = \frac{2}{\theta_3(e^{-\gamma}) - 1}. \quad (74)$$

In the general case of arbitrary $b > 0$, the asymptotic behaviors of the sums in Eqs. (71) and (72) can be established when $\gamma \to 0^+$. In this situation, we replace the summation by integration and arrive at the following leading behaviors:

$$\lambda_c \simeq \frac{\gamma^{1/b}}{\Gamma\left(1 + \frac{1}{b}\right)}, \qquad D \simeq 2\frac{\Gamma^2\left(1 + \frac{1}{b}\right)}{\Gamma\left(1 + \frac{2}{b}\right)}. \quad (75)$$

The number of newly infected individuals follows different scaling behaviors depending on whether $b > 1$ or $b < 1$. The kernel $F(\tau)$ decays faster than exponential if $b > 1$, so the generating function $G_{\gamma,b}(x)$ has an infinite radius of convergence in this situation, and $n(t)$ follows Eq. (15). The growth rate μ is determined by Eq. (14) that for the kernel (68) becomes

$$\lambda G_{\gamma,b}(e^{-\mu}) = 1. \quad (76)$$

In Fig. 6, we show numerical results for the number of newly infected individuals for $b = 1.25 > 1$ in the supercritical, critical, and subcritical regimes. The total number $N(t)$ of infected individuals for $b > 1$ follows Eq. (17) for any value of λ with μ given by Eq. (76).

When $b < 1$, the kernel $F(\tau)$ decays slower than exponential, and the radius of convergence of $G_{\gamma,b}(x)$ is $R = 1$. Therefore, we might expect deviations from the exponential scaling described by Eq. (15) in the critical and subcritical regimes. Here, we summarize the asymptotic behaviors in these regimes (see Appendix C for the derivations). In the critical regime, the asymptotic analysis shows that the number of newly infected individuals $n(t)$ saturates asymptotically for long times t (see Fig. 6) with the limit given by

$$\lim_{t \to \infty} n(t) = \frac{G_{\gamma,b}(1)}{G'_{\gamma,b}(1)}. \quad (77)$$

Therefore, in the critical regime, the total number $N(t)$ of infected individuals grows linearly with time for $t \gg 1$.

In the subcritical regime, the asymptotic scaling analysis (see Appendix C) implies that $n(t)$ decays faster than t^{-2}. Our numerical analysis indicates that $n(t)$ decays, such as $F(t)$, see Fig. 6(c). Therefore, in the subcritical regime, the total number $N(t)$ of infected individuals for sufficiently long times saturates to a constant value. The scalings of the total number $N(t)$ of infected individuals in the supercritical, critical and subcritical regime are summarized in Table II.

VIII. MULTIFOCI SI MODEL

An epidemic outbreak in one region of the world can spread to other regions also in the presence of containment measures forming several foci of the epidemics. We, thus, consider a model in which the pandemic is formed by a set of separated foci i where the outbreak starts at different times t_i. A realistic metapopulation model of this sort may account for the mobility of the individuals across the different locations utilizing transportation networks. Here, we employ a simplified mean-field approach and assume that the number of new foci at time $t = t_i$ is a deterministic function of t_i indicated by $\rho(t_i)$. We consider two functional forms for $\rho(t_i)$:

(A) A power-law functional form for $\rho(t_i)$,

$$\rho(t_i) = Bt_i^\gamma, \quad (78)$$

where $\gamma \geqslant 0$ and $B > 0$. A constant number of new foci as a function of time corresponds to $\gamma = 0$; if $\gamma > 0$, the number of new foci increases with time.

(B) An exponential functional form for $\rho(t_i)$,

$$\rho(t_i) = Be^{\theta t_i}, \tag{79}$$

with $\theta \geqslant 0$ and $B > 0$. If $\theta > 0$, the number of new foci increases exponentially as a function of time.

In both scenarios, the total number of cases $I(t)$ at time t calculated across all the foci is given by

$$I(t) = \sum_1^{t-1} N_i(t - t_i)\rho(t_i), \tag{80}$$

where $N_i(t - t_i)$ is the total number of cases of the foci i at time t. In principle, at every foci, different containment measures could be applied, but we focus on the simplest situation when each focus follows the same dynamics and has the same parameters.

IX. TOTAL NUMBER OF INFECTED IN THE MULTIFOCI MODEL

In this section, we calculate the total number of infected individuals $I(t)$ in the multifoci metapopulation approach. Since we assume that every foci follows the same dynamics, $I(t)$ is given by Eq. (80) with N_i being the same and just shifted to the activation time t_i, that is $N_i(t - t_i) = N(t - t_i)$ at time t.

For the kernels which we employ, the asymptotic behavior of $N(t)$ at long times can be cast in two major classes: the exponential behavior and the power-law behavior. We now separately consider these two cases.

A. Exponential case

Consider an exponential dependence of $N(t)$, i.e.,

$$N(t) \simeq Ce^{\mu t}, \tag{81}$$

where, without loss of generality, we consider $\mu > 0$.

(A) If the number of new foci increases as a power law Eq. (78), by putting Eq. (81) into Eq. (80) and limiting ourselves to the situation when the growth of $N(t)$ is exponential $\mu > 0$, we obtain

$$I(t) \simeq \mathcal{C} \operatorname{Li}_{-\gamma}(e^{-\mu})e^{\mu t}, \tag{82}$$

where $\mathcal{C} = BC$ and where $\operatorname{Li}_a(x)$ is a polylogarithm with index a. Therefore, for $\mu > 0$, the presence of different foci does not change the exponential trend and $I(t)$ and $N(t)$ differ only by a constant.

(B) If the number of new foci increases exponentially Eq. (79), we put Eq. (81) into Eq. (80) to yield

$$I(t) \simeq \begin{cases} \mathcal{C}e^{\mu t}, & \text{if } \mu > \theta, \\ \mathcal{C}te^{\mu t}, & \text{if } \mu = \theta, \\ \mathcal{C}e^{\theta t}[e^{\theta - \mu} - 1]^{-1}, & \text{if } \mu < \theta, \end{cases} \tag{83}$$

where $\mathcal{C} = BC$. Thus, the presence of different foci changes the exponential trends if and only if $\theta \geqslant \mu$.

B. Power-law case

We, now, consider the case in which the total number of infected individuals $N(t)$ in each focus of the epidemics scales as a power law,

$$N(t) = Ct^\nu \tag{84}$$

for $t \gg 1$. We can assume that $\nu \geqslant 0$. Indeed, the definition of the total number $N(t)$ of infected individuals in a given focus, given by Eq. (5) implies that $N(t)$ is a nondecreasing function of time with $N(t) \geqslant n(0) = 1$.

(A) We now insert Eq. (84) into Eq. (80) and approximate the sum by an integral in the long time limit. Computing the integral, we obtain

$$I(t) \simeq C B(1 + \gamma, 1 + \nu)t^{1 + \gamma + \nu}, \tag{85}$$

where $B(a, b)$ is the Euler β function,

$$B(a, b) = \int_0^1 dx \, x^{a-1}(1 - x)^{b-1}. \tag{86}$$

The replacement of the sum by an integral is asymptotically justifiable when $\gamma > -1$. Note that both $I(t)$ and $N(t)$ grow algebraically. The presence of different foci *accelerates* the growth $1 + \gamma + \nu > \nu$ when $\gamma > -1$. If $\gamma \leqslant -1$, we estimate the sum in Eq. (80) more carefully and get

$$I(t) \simeq Ct^\nu \times \begin{cases} \ln t, & \gamma = -1, \\ \zeta(-\gamma), & \gamma < -1. \end{cases} \tag{87}$$

(B) If the number of new foci increases exponentially, Eq. (79), we put Eq. (84) into Eq. (80) to yield

$$I(t) \simeq \mathcal{C} \operatorname{Li}_{-\nu}(e^{-\theta})e^{\theta t}, \tag{88}$$

where $\mathcal{C} = BC$ and the polylogarithm function $\operatorname{Li}_a(x)$ is defined in Eq. (34). Therefore, in this case, the total number of infected across all the foci is growing exponentially with rate θ. In other words, $I(t)$ growth in time is dominated by the rate at which new foci are established.

X. CONCLUSIONS

We proposed an epidemic model with time-dependent infectivity that mimics different types of containment measures. This model allows one to study the onset of epidemics and the role that time-dependent infectivity can have on the spread of the disease. We demonstrated that different containment measures can either lead to a slowing down of the exponential spread by modulating the growth rate μ or can bring the epidemic to a halt when they push the dynamics in the subcritical regime. In particular, exponential and generalized exponential temporal kernels always induce a finite epidemic threshold λ_c, so they stop epidemics provided that $\lambda < \lambda_c$. Sufficiently steep power-law temporal kernels also induce a nonvanishing epidemic threshold—this happens when the decay exponent characterizing the kernel satisfied exceeds unity: $\alpha > 1$. In the supercritical regime, $\lambda > \lambda_c$, the total number of infected individuals grows exponentially with a characteristic timescale that diverges at the critical point following different universality classes depending on the kernel; in the subcritical regime, the total number of infected individuals saturates to a constant; in the critical regime, the number of infected

individuals grows in time linearly or sublinearly. These results have been obtained assuming a well-mixed approximation and by considering a single focus of the epidemic.

We also briefly investigated the multifoci version in the simplest situation when each focus follows the same dynamics. We showed that if the number of new foci increases as a power law of time, in the supercritical regime the total number of cases across different foci scales, such as the total number of cases in each focus. In the critical and subcritical regimes, the total number of cases across different foci can grow faster than linearly. Qualitatively different behaviors emerge also in the supercritical regime when the number of new foci increases exponentially with rate exceeding the "bare" rate μ.

There are many avenues for future work. An obvious important challenge is to model stochastic characteristics and account for large fluctuations observed in pandemics. Stochastic characteristics are difficult to describe even in the classical SIR model in the critical regime [39–46], and they may play an important role in our model. Finally, the multifoci metapopulation approach could be expanded by considering the effect of social and transportation networks.

ACKNOWLEDGMENTS

APPENDIX A: DERIVATION OF EQ. (56)

In this Appendix, we derive the announced asymptotic behaviors (56) of the number of new infected individual $n(t)$ in the critical regime for the power-law kernel. We also derive the predictions (57) for the amplitude, and compute the subleading term in the special case of $\alpha = 2$ when the convergence to the leading asymptotic is anomalously slow.

Our starting point is Eq. (35) that we rewrite as

$$\mathcal{N}(x) = \frac{1}{1 - \lambda_c \mathrm{Li}_\alpha(x)}. \tag{A1}$$

We keep in mind known relations $\lambda = \lambda_c = 1/\zeta(\alpha)$ characterizing the critical regime of the power-law kernel in the $\alpha > 1$ range.

To establish Eq. (56), we expand the right-hand side of Eq. (A1) in the region $x \to 1^-$; the asymptotic behavior of $n(t)$ follows from this expansion. The polylogarithmic function $\mathrm{Li}_\alpha(x)$ exhibits different asymptotic behaviors in the $x \to 1^-$ limit depending on whether different values of α is smaller or larger than 2. Therefore, we separately treat the cases of $1 < \alpha < 2$, $\alpha = 2$, and $\alpha > 2$.

1. The case of $1 < \alpha < 2$

In this range, the polylogarithmic function $\mathrm{Li}_\alpha(x)$ admits the asymptotic expansion (50) which we insert into Eq. (A1) and arrive at

$$\mathcal{N}(x) \simeq -\frac{\zeta(\alpha)}{\Gamma(1-\alpha)}(1-x)^{1-\alpha}, \tag{A2}$$

as $x \to 1^-$. Thus,

$$\sum_{t \geqslant 0} n(t)x^t \simeq -\frac{\zeta(\alpha)}{\Gamma(1-\alpha)}(1-x)^{1-\alpha}, \tag{A3}$$

which implies the long-time behavior,

$$n(t) \simeq -\frac{\zeta(\alpha)}{\Gamma(\alpha-1)\Gamma(1-\alpha)}t^{\alpha-2} \tag{A4}$$

stated in Eqs. (56) and (57) when $1 < \alpha < 2$. Using the Euler identity $\Gamma(y)\Gamma(1-y) = \pi / \sin(\pi y)$, one can also rewrite (A4) as

$$n(t) \simeq \frac{(\alpha-1)\zeta(\alpha)\sin[\pi(\alpha-1)]}{\pi}t^{\alpha-2}. \tag{A5}$$

As a simple "physical" confirmation of Eq. (A4), one can substitute Eq. (A4) into the sum on the left-hand side of Eq. (A2), note that in the $x \to 1^-$ limit the summation can be replaced by integration; computing the integral, one recovers the right-hand side of (A2). A rigorous derivation of the asymptotic of the coefficients from the singular behavior of the generating function can be performed by a variety of techniques, e.g., by using Tauberian theorems [49] or complex analysis [50]; see the textbook [51] for numerous examples.

2. The case of $\alpha = 2$

The polylogarithmic function $\mathrm{Li}_2(x)$ has the asymptotic expansion (52) which we insert into Eq. (A1) and obtain

$$\mathcal{N}(x) \simeq \frac{\zeta(2)}{1-\ln(1-x)}\frac{1}{1-x}, \tag{A6}$$

from which we deduce the leading asymptotic behavior reported in (56) and (57) at $\alpha = 2$. The presence of logarithms often implies that the subleading term is just logarithmically smaller than the leading term, and, then, the sub-sub-leading term is another logarithmic factor smaller. The derivation of these subleading terms is a bit long, but it uses standard techniques [50,51]; alternatively, it can be also extracted from the general results presented in Ref. [51]. Keeping just the leading and subleading terms yield the following asymptotic:

$$n(t) \simeq \frac{\zeta(2)}{\ln t + \gamma_E + 1}, \tag{A7}$$

where γ_E is the Euler-Mascheroni constant and we have dropped the terms of the order $(\ln t)^{-3}$. Using Eq. (A7), we obtain a slightly more precise version of Eq. (58) at $\alpha = 2$,

$$N(t) \simeq \frac{\zeta(2)t}{\ln t + \gamma_E}. \tag{A8}$$

3. The case of $\alpha > 2$

When $\alpha > 2$, the polylogarithmic function $\mathrm{Li}_\alpha(x)$ admits the asymptotic expansion (54) which we insert into (A1) and get

$$\mathcal{N}(x) \simeq \frac{\zeta(\alpha)}{\zeta(\alpha-1)}(1-x)^{-1}, \tag{A9}$$

implying that the number $n(t)$ of new infected individuals saturates

$$\lim_{t \to \infty} n(t) = \frac{\zeta(\alpha)}{\zeta(\alpha-1)}, \tag{A10}$$

as stated in Eqs. (56) and (57) at $\alpha > 2$.

APPENDIX B: DERIVATION OF EQ. (60)

In this Appendix, we derive the announced asymptotic behavior (60) applicable in the subcritical regime. We start with Eq. (35) that we rewrite, here, for convenience,

$$\mathcal{N}(x) = \frac{1}{1 - \lambda \operatorname{Li}_\alpha(x)}. \qquad \text{(B1)}$$

The subcritical regime $\lambda < \lambda_c = 1/\zeta(\alpha)$ is possible for all $\alpha > 1$. Since $\mathcal{N}(1)$ is finite, we consider the expansion of $\mathcal{N}(1) - \mathcal{N}(x)$ in the $x \to 1^-$ limit. By using Eq. (B1), one can derive the asymptotic expression of $n(t)$ in the range of $1 < \alpha \leqslant 2$. This is carried out below first when $1 < \alpha < 2$ and, then, at $\alpha = 2$. In these cases, we recover the asymptotic scaling in Eq. (60). The same method, in principle, applies to all $\alpha > 2$, but our treatment is less rigorous there as it is based on the analysis the $2 < \alpha < 3$ range than the $3 < \alpha < 4$ range, etc., and it quickly becomes cumbersome.

1. The case of $1 < \alpha < 2$

In the $1 < \alpha < 2$ range, the deviation of $\operatorname{Li}_\alpha(x)$ from $\operatorname{Li}_\alpha(1) = \zeta(\alpha)$ scales as

$$\operatorname{Li}_\alpha(x) - \operatorname{Li}_\alpha(1) \simeq \Gamma(1 - \alpha)(1 - x)^{\alpha - 1}, \qquad \text{(B2)}$$

when $x \to 1^-$. This is just the rewriting of Eq. (50). Using Eqs. (B1) and (B2), we find

$$\mathcal{N}(1) - \mathcal{N}(x) \simeq -\frac{\lambda \Gamma(1 - \alpha)}{[1 - \lambda \zeta(\alpha)]^2}(1 - x)^{\alpha - 1}. \qquad \text{(B3)}$$

Recalling the definition of the generating function $\mathcal{N}(x)$, we get

$$\sum_{t \geqslant 0} n(t)[1 - x^t] \simeq -\frac{\lambda \Gamma(1 - \alpha)}{[1 - \lambda \zeta(\alpha)]^2}(1 - x)^{\alpha - 1}. \qquad \text{(B4)}$$

Differentiating with respect to x to obtain

$$\sum_{t \geqslant 0} tn(t)x^{t-1} \simeq (1 - x)^{\alpha - 2}\frac{\lambda \Gamma(2 - \alpha)}{[1 - \lambda \zeta(\alpha)]^2} \qquad \text{(B5)}$$

leading to the announced asymptotic behavior (60) in the $1 < \alpha < 2$ range.

2. The case of $\alpha = 2$

When $\alpha = 2$, we rewrite (52) as

$$\operatorname{Li}_2(1) - \operatorname{Li}_2(x) \simeq (1 - x)[\ln(1 - x) - 1]. \qquad \text{(B6)}$$

Using Eqs. (B1) and (B6), we find

$$\mathcal{N}(1) - \mathcal{N}(x) \simeq (1 - x)[\ln(1 - x) - 1]\frac{\lambda}{[1 - \lambda \zeta(2)]^2}, \qquad \text{(B7)}$$

from which we deduce

$$\sum_{t \geqslant 0} tn(t)x^{t-1} \simeq -\ln(1 - x)\frac{\lambda}{[1 - \lambda \zeta(2)]^2} \qquad \text{(B8)}$$

leading to the announced asymptotic (60) at $\alpha = 2$.

3. The case of $\alpha > 2$

For $\alpha > 2$, we rewrite Eq. (54) as

$$\operatorname{Li}_\alpha(1) - \operatorname{Li}_\alpha(x) \simeq \zeta(\alpha - 1)(1 - x). \qquad \text{(B9)}$$

Using Eqs. (B1) and (B9), we find

$$\mathcal{N}(1) - \mathcal{N}(x) \simeq \frac{\lambda \zeta(\alpha - 1)}{[1 - \lambda \zeta(\alpha)]^2}(1 - x). \qquad \text{(B10)}$$

The same treatment as before gives

$$\sum_{t \geqslant 0} tn(t) = \frac{\lambda \zeta(\alpha - 1)}{[1 - \lambda \zeta(\alpha)]^2}, \qquad \text{(B11)}$$

which only implies that $n(t)$ should decay faster than t^{-2}.

To derive the announced asymptotic (60) for $\alpha > 2$, one should employ the expansion of $\operatorname{Li}_\alpha(1) - \operatorname{Li}_\alpha(x)$ which is more accurate than the leading term given by Eq. (B9). Let us first consider the region $2 < \alpha < 3$. In this range, the required more accurate form reads

$$\operatorname{Li}_\alpha(1) - \operatorname{Li}_\alpha(x) = \zeta(\alpha - 1)(1 - x) - B(1 - x)^{\alpha - 1} + \cdots. \qquad \text{(B12)}$$

Differentiating Eq. (B12) twice with respect of x and using the identity,

$$\frac{d^2 \operatorname{Li}_\alpha(x)}{dx^2} = \frac{\operatorname{Li}_{\alpha - 2}(x) - \operatorname{Li}_{\alpha - 1}(x)}{x^2} \qquad \text{(B13)}$$

we obtain

$$\operatorname{Li}_{\alpha - 2}(x) - \operatorname{Li}_{\alpha - 1}(x) \simeq B(\alpha - 1)(\alpha - 2)(1 - x)^{\alpha - 3} \qquad \text{(B14)}$$

in the $x \to 1^-$ limit. The leading behavior of the left-hand side of Eq. (B14) is provided by the leading asymptotic of $\operatorname{Li}_{\alpha - 2}(x)$, and it reads

$$\operatorname{Li}_{\alpha - 2}(x) \simeq \Gamma(3 - \alpha)(1 - x)^{\alpha - 3}. \qquad \text{(B15)}$$

Thus, we fix the amplitude in (B14),

$$B = \frac{\Gamma(3 - \alpha)}{(\alpha - 1)(\alpha - 2)}. \qquad \text{(B16)}$$

Using Eqs. (B1) and (B9), we obtain

$$\sum_{t \geqslant 0} n(t)[1 - x^t] \simeq \frac{\lambda \zeta(\alpha - 1)}{[1 - \lambda \zeta(\alpha)]^2}(1 - x)$$
$$- \frac{\lambda}{[1 - \lambda \zeta(\alpha)]^2}B(1 - x)^{\alpha - 1},$$

which we differentiate twice with respect to x to yield

$$\sum_{t \geqslant 0} t(t - 1)n(t)x^{t-2} \simeq (1 - x)^{\alpha - 3}\frac{\lambda \Gamma(3 - \alpha)}{[1 - \lambda \zeta(\alpha)]^2}, \qquad \text{(B17)}$$

where we have also used Eq. (B16). From the above expression, we confirm the announced asymptotic (60) in the range of $2 < \alpha < 3$. The same tedious analysis using allows one to confirm Eq. (60) at $\alpha = 3$. In the range of $3 < \alpha < 4$, one needs to use an extra term,

$$\operatorname{Li}_\alpha(1) - \operatorname{Li}_\alpha(x) = \zeta(\alpha - 1)(1 - x) + B_2(1 - x)^2$$
$$- B_3(1 - x)^{\alpha - 1} + \cdots. \qquad \text{(B18)}$$

The most important is the singular term $B_3(1-x)^{\alpha-1}$, with amplitude B_3 found after differentiating Eq. (B18) three times with respect of x. One, then, obtains

$$\sum_{t \geqslant 0} t(t-1)(t-3)n(t)x^{t-2} \sim (1-x)^{\alpha-4}, \qquad (B19)$$

from which one confirms Eq. (60) in the range of $3 < \alpha < 4$.

The above tedious proof extends to all $\alpha > 2$. The simplicity of the final result Eq. (60), hints on a possible general derivation circumventing the consideration of the infinitely many intervals $k < \alpha < k+1$ for all integers $k \geqslant 1$, and the separate analysis of $\alpha = k$ with $k \geqslant 2$ where the logarithms arise in the intermediate steps but disappear from the final formula given by Eq. (60).

APPENDIX C: ASYMPTOTIC ANALYSIS OF THE GENERALIZED EXPONENTIAL KERNEL WITH $b < 1$

In this Appendix, we discuss the derivation of the asymptotic expansion for $n(t)$ for the generalized exponential kernel with $b < 1$. In the critical regime, the generating function $\mathcal{N}(x)$ satisfies

$$\mathcal{N}(x) = \frac{1}{1 - \lambda_c G_{\gamma,b}(x)}. \qquad (C1)$$

In the $x \to 1^-$ limit, we, therefore, obtain

$$\mathcal{N}(x) \simeq \frac{G_{\gamma,b}(1)}{G'_{\gamma,b}(1)}(1-x)^{-1}, \qquad (C2)$$

leading to the asymptotic behavior (77), namely,

$$\lim_{t \to \infty} n(t) = \frac{G_{\gamma,b}(1)}{G'_{\gamma,b}(1)}. \qquad (C3)$$

In the subcritical regime, $\lambda < \lambda_c$, we obtain

$$\mathcal{N}(1) - \mathcal{N}(x) \simeq \frac{\lambda\, G'_{\gamma,b}(1)}{[1 - \lambda G_{\gamma,b}(1)]^2}(1-x), \qquad (C4)$$

as $x \to 1^-$, which we treat as in Appendix B and find

$$\sum_{t \geqslant 1} tn(t) = C_1 \equiv \frac{\lambda G'_{\gamma,b}(1)}{[1 - \lambda G_{\gamma,b}(1)]^2} \qquad (C5)$$

telling us that $n(t)$ decays faster than t^{-2}.

To derive a more precise prediction one can use the same trick as in Appendix B, namely to establish a more precise expansion than Eq. (C4). One gets, however, the regular expansion,

$$\mathcal{N}(1) - \mathcal{N}(x) \simeq C_1(1-x) + \tfrac{1}{2}C_2(1-x)^2 + \tfrac{1}{6}C_3(1-x)^3 + \cdots,$$

from which

$$\sum_{t \geqslant 1} t(t-1)n(t) = C_2, \qquad \sum_{t \geqslant 1} t(t-1)(t-2)n(t) = C_3,$$

etc. The first sum rule implies that $n(t)$ decays faster than t^{-3}, the second tells us that $n(t)$ decays faster than t^{-4}. Proceeding, one finds that $n(t)$ seemingly decays faster than any power of time. Recall, that for the power-law kernel, the decay of $n(t)$ in the subcritical regime is qualitatively the same as the decay of the kernel $F(\tau)$. This may occur also for the generalized exponential kernel, and our simulation results agree with this conjecture. Theoretically, however, we only established that the decay of $n(t)$ is faster than any power law.

[1] M. Chinazzi *et al.*, Science **368**, 395 (2020).

[2] B. F. Maier and D. Brockmann, Science **368**, 742 (2020).

[3] S. Maslov and N. Goldenfeld, arXiv:2003.09564.

[4] L. Ferretti, C. Wymant, M. Kendall, L. Zhao, A. Nurtay, D. G. Bonsall, and C. Fraser, Science **368**, eabb6936 (2020).

[5] Y. Liu, H. Sanhedrai, G. Dong, L. M. Shekhtman, F. Wang, S. V. Buldyrev, and S. Havlin, Nat. Sci. Rev., nwaa229 (2020).

[6] V. Zlatić, I. Barjašić, A. Kadović, H. Štefančić, and A. Gabrielli, Nonlinear Dyn. (2020).

[7] G. Bianconi, H. Sun, G. Rapisardi, and A. Arenas, arXiv:2007.05277.

[8] A. L. Ziff and R. M. Ziff, doi: 10.1101/2020.02.16.20023820.

[9] B. Gross, Z. Zheng, S. Liu, X. Chen, A. Sela, J. Li, D. Li, and S. Havlin, arXiv:2003.08382.

[10] M. McNeill, *Plagues and People* (Anchor, New York, 1989).

[11] M. Oldstone, *Viruses, Plagues, and History* (Oxford University Press, Oxford, 1998).

[12] D. Bernoulli, Mem. Math. Phys. Acad. Roy. Sci. **1**, 1 (1766).

[13] A. S. Perelson and P. W. Nelson, SIAM Rev **41**, 3 (1999).

[14] M. A. Nowak and R. May, *Virus Dynamics: Mathematical Principles of Immunology and Virology* (Oxford University Press, Oxford, 2001).

[15] F. Radicchi and G. Bianconi, arXiv:2007.15034.

[16] O. Valba, V. Avetisov, A. Gorsky, and S. Nechaev, Phys. Rev. E **102**, 010401(R) (2020).

[17] L. Dell'Anna, arXiv:2003.13571.

[18] M. Vrugt, J. Bickmann, and R. Wittkowski, arXiv:2003.13967.

[19] B. Blasius, arXiv:2004.00940.

[20] M. A. Ludwig, *The Giant Black Book of Computer Viruses* (American Eagle Show Low, AZ, 1998).

[21] E. M. Rogers, *Diffusion of Innovations* (Free, New York, 2003).

[22] M. Nekovee, Y. Moreno, G. Bianconi, and M. Marsili, Physica A **374**, 457 (2007).

[23] C. Castellano, S. Fortunato, and V. Loreto, Rev. Mod. Phys. **81**, 591 (2009).

[24] M. A. Amaral, W. G. Dantas, and J. J. Arenzon, Phys. Rev. E **101**, 062418 (2020).

[25] N. T. J. Bailey, *The Mathematical Theory of Epidemics* (Hafner, New York, 1957).

[26] N. T. J. Bailey, *The Mathematical Theory of Infectious Diseases* (Oxford University Press, Oxford, 1987).

[27] R. Anderson and R. May, *Infectious Diseases: Dynamics and Control* (Oxford University Press, Oxford, 1991).

[28] H. Andersson and T. Britton, *Stochastic Epidemic Models and Their Statistical Analysis* (Springer, New York, 2000).

[29] J. D. Murray, *Mathematical Biology: I. An Introduction* (Springer, New York, 2007), Vol. 17.

[30] P. L. Krapivsky, S. Redner, and E. Ben-Naim, *A Kinetic View of Statistical Physics* (Cambridge University Press, Cambridge, UK, 2010).

[31] A.-L. Barabási *et al.*, *Network Science* (Cambridge University Press, Cambridge, UK, 2016).

[32] M. Newman, *Networks* (Oxford University Press, Oxford, 2010).

[33] G. Bianconi, *Multilayer Networks: Structure and Function* (Oxford University Press, Oxford, 2018).

[34] S. N. Dorogovtsev, *Lectures on Complex Networks* (Oxford University Press, Oxford, 2010), Vol. 24.

[35] R. Pastor-Satorras, C. Castellano, P. Van Mieghem, and A. Vespignani, Rev. Mod. Phys. **87**, 925 (2015).

[36] H. W. Hethcote, SIAM Rev. **42**, 599 (2000).

[37] V. Colizza, R. Pastor-Satorras, and A. Vespignani, Nat. Phys. **3**, 276 (2007).

[38] V. Colizza, A. Barrat, M. Barthelemy, A.-J. Valleron, and A. Vespignani, PLoS Med. **4**, e13 (2007).

[39] A. Martin-Löf, J. Appl. Probab. **35**, 671 (1998).

[40] E. Ben-Naim and P. L. Krapivsky, Phys. Rev. E **69**, 050901(R) (2004).

[41] D. A. Kessler and N. M. Shnerb, Phys. Rev. E **76**, 010901(R) (2007).

[42] D. A. Kessler, J. Appl. Probab. **45**, 757 (2008).

[43] L. F. Gordillo, S. A. Marion, A. Martin-Löf, and P. E. Greenwood, Bull. Math. Biol. **70**, 589 (2008).

[44] E. Ben-Naim and P. Krapivsky, Eur. Phys. J. B **85**, 145 (2012).

[45] T. Antal and P. L. Krapivsky, J. Stat. Mech. (2014) P07018.

[46] I. Kortchemski, Stoch. Process Appl. **125**, 886 (2015).

[47] J. Stehlé, N. Voirin, A. Barrat, C. Cattuto, L. Isella, J.-F. Pinton, M. Quaggiotto, W. Van den Broeck, C. Régis, B. Lina *et al.*, PloS One **6**, e23176 (2011).

[48] P. Vanhems, A. Barrat, C. Cattuto, J.-F. Pinton, N. Khanafer, C. Régis, B.-a. Kim, B. Comte, and N. Voirin, PloS One **8**, e73970 (2013).

[49] G. H. Hardy, *Divergent Series* (Clarendon, Oxford, 1967).

[50] P. Flajolet and A. M. Odlyzko, SIAM J. Discrete Math. **3**, 216 (1990).

[51] P. Flajolet and R. Sedgewick, *Analytic Combinatorics* (Cambridge University Press, Cambridge, UK, 2009).